THE JOURNAL OF BIOLOGICAL CHEMISTRY VOL. 285, NO. 27, pp. 21013–21022, July 2, 2010

ZF21 Protein Regulates Cell Adhesion and Motility*[S]

Received for publication, January 21, 2010, and in revised form, April 2, 2010 Published, JBC Papers in Press, May 3, 2010, DOI 10.1074/jbc.M110.106443

Makoto Nagano, Daisuke Hoshino, Takeharu Sakamoto, Noritaka Kawasaki, Naohiko Koshikawa, and Motoharu Seiki[1]

From the Division of Cancer Cell Research, Institute of Medical Science, University of Tokyo, Shirokanedai, Minato-ku, Tokyo 108-8639, Japan

Cell migration on an extracellular matrix (ECM) requires continuous formation and turnover of focal adhesions (FAs) along the direction of cell movement. However, our knowledge of the components of FAs and the mechanism of their regulation remains limited. Here, we identify ZF21, a member of a protein family characterized by the presence of a phosphatidylinositol 3-phosphate-binding FYVE domain, to be a new regulator of FAs and cell movement. Knockdown of ZF21 expression in cells increased the number of FAs and suppressed cell migration. Knockdown of ZF21 expression also led to a significant delay in FA disassembly following induction of synchronous disassembly of FAs by nocodazole treatment. ZF21 bound to focal adhesion kinase, localized to FAs, and was necessary for dephosphorylation of FAK at Tyr^{397}, which is important for disassembly of FAs. Thus, ZF21 represents a new component of FAs, mediates disassembly of FAs, and thereby regulates cell motility.

The cells in most tissues are surrounded by an extracellular matrix (ECM),[2] and interaction of the cells with the ECM plays a pivotal role in maintaining cell morphology and tissue architecture and in mediating signals regulating a variety of cellular functions, such as proliferation, motility, survival, and differentiation (1–3). Integrins are the major receptors for proteins of the ECM and they transmit ECM-mediated signals to a variety of intracellular machineries (4). Binding of cells to the ECM induces clustering of integrins and triggers recruitment of multiple cellular proteins to the inner surface of the plasma membrane (4, 5). Formation and reorganization of such adhesion structures are particularly important for cell migration, and these structures are regulated dynamically along the direction of cell movement (6, 7). The formation of adhesion structures during the spreading and migration of cultured cells on ECM layers has been studied extensively (8, 9). During cell migration, primitive adhesion structures can be observed at the migration front as relatively small focal complexes along the periphery of ruffling membranes (10). Most of these structures are short lived, but some grow to become more stable adhesion links to the actin cytoskeleton so as to permit the generation of force for cell movement via actin contraction (10, 11). Activation of Rho/ROCK signals at the adhesion complex promotes actin polymerization and leads to the development of mature focal adhesions (FAs) (12). Although the formation of FAs at the migration front is important for the generation of a driving force to pull the cell body forward, the FAs gradually migrate to the rear of the cell because of movement of the cell body. To continue migration forward, these FAs at the rear must be disassembled to allow detachment from the ECM. Thus, it is important to understand how formation and disassembly of FAs are regulated during cell migration.

Multiple cellular proteins are recruited to the cytoplasmic domains of integrins, where they mediate both physical connection to the cytoskeleton and functional connections to cellular signaling pathways (13). These cytoplasmic effectors include Paxillin, Vinculin, α-actinin, and Talin, which together act as a scaffold to connect integrins to the cytoskeleton (13–17). Clustering of integrins leads to successive phosphorylation of FAK, c-Src, and adaptor proteins, such as p130Cas and CrkII at FAs (18–21). Activation of the Rho/ROCK cascade stimulates formation of stress fibers that stabilize the adhesion structures, which mature into stable FAs (12, 22).

Although our knowledge of the processes regulating the assembly of FAs has accumulated, the regulation of their disassembly remains less well understood. However, previous studies have revealed that extension of microtubules to FAs is essential to initiate their disassembly and that disruption of microtubules by treatment of cells with nocodazole stabilizes FA structures (23–25). Treatment of cells with nocodazole and subsequent retraction of the drug from the culture media triggers synchronous disassembly of FAs. Therefore, nocodazole is an excellent tool to dissect the steps of FA assembly and disassembly. Calpain-2, a calcium-dependent endopeptidase, has been implicated in the destruction of FAs via cleavage of integrin, FAK, Talin, and α-actinin, etc. (26). Dephosphorylation of FAK, Paxillin, and p130CAS by protein-tyrosine phosphatases, such as PTP-PEST, SHP-2, or PTP-1B, also induces disassembly of FA complexes (27–29). At the final stage of FA disassembly, integrins are internalized in a dynamin-dependent manner (23, 30). However, it is apparent that such information explains only a portion of the full process of disassembly of FAs.

* This work was supported by the Specific Coordination Fund for Promoting Science (to T. S.), by a grant-in-aid for scientific research on priority areas ("Integrative Research toward the Conquest of Cancer") (to M. S.), and by Global COE Program (to T. S. and M. S.) from the Ministry of Education, Culture, Sports, Science and Technology of Japan.

[S] The on-line version of this article (available at http://www.jbc.org) contains supplemental Fig. S1.

[1] To whom correspondence should be addressed: 4-6-1 Shirokanedai, Minato-ku, Tokyo 108-8639, Japan. Fax: 81-3-5449-5414; E-mail: mseiki@ims.u-tokyo.ac.jp.

[2] The abbreviations used are: ECM, extracellular matrix; EEA1, Early endosome antigen 1; FYVE, Fab1p YOPB Vps27p, EEA1; FA, focal adhesion; ZF21, ZFYVE21; FAK, focal adhesion kinase; PIPES, 1,4-piperazinediethanesulfonic acid; DMEM, Dulbecco's modified Eagle's medium; GST, glutathione *S*-transferase; PBS, phosphate-buffered saline; shRNA, small hairpin RNA; TIRF, total internal reflection fluorescence; WT, wild type.

In this study, we identify ZFYVE21 (ZF21) to be a new constituent protein of FAs that acts as a key regulator of their disassembly. We previously identified ZF21 as a protein that could bind to the cytoplasmic tail of membrane type 1 matrix metalloproteinase (31), a potent invasion-promoting protease (32). A cDNA fragment encoding ZF21 was isolated as a result of a yeast two-hybrid screen using the cytoplasmic tail as bait (31), although the interaction may not represent a physiological one because we were unable to detect direct binding of ZF21 to membrane type 1 matrix metalloproteinase *in vitro* or *in vivo*.[3] During that study, however, we observed that ZF21 could modulate cell adhesion. We show here that knockdown of ZF21 expression enhances adhesion of cells to the ECM and that it suppresses their migration. We also show that ZF21 is required to initiate the disassembly of FAs. Finally, we demonstrate that ZF21 localizes to FAs, where it can bind and prevent the dephosphorylation of FAK.

EXPERIMENTAL PROCEDURES

Cell Cultures—HT1080, MDA-MB231, and COS-1 cells were obtained from the American Type Culture Collection (Manassas, VA). Cells were cultured in DMEM (Invitrogen), supplemented with 10% fetal bovine serum, penicillin, and streptomycin (Invitrogen). All cells were cultured at 37 °C under a 5% CO_2, 95% air atmosphere.

Antibodies and Reagents—A polyclonal anti-ZF21 antibody was prepared by affinity purification of immune sera collected following the immunization of a rabbit or a chicken with the recombinant protein expressed in *Escherichia coli*. We used commercially available antibodies to detect Myc (Roche Applied Science), EEA1 (14) (BD Biosciences), transferrin receptor (H68.4, Zymed Laboratories Inc.), β-tubulin (E7, Development Studies Hybridoma Bank), Venus (anti-GFP, A11122, Invitrogen), actin (C4, Millipore), integrin-β1 (18) (BD Biosciences), integrin-β1 for adhesion blocking (6S6, Millipore), FAK (BD Biosciences), Tyr^{397}-phosphorylated FAK (BIOSOURCE or Abcam), Vinculin (VIN-11–5, Sigma), Talin (8D4, Sigma), SHP-2, and PTP-1B (PTP sampler kit, BD Bioscience). Nocodazole (Sigma) was used at 5 μM. Type I-A collagen was purchased from Nitta Gelatin. All other chemical reagents were purchased from Sigma or Wako, unless otherwise indicated.

Plasmids—cDNAs encoding ZFYVE21 (ZF21), FAK, Paxillin, Zyxin, SHP-2, or PTP-1B were amplified from HT1080 cells by reverse transcription-PCR. ZF21 mutants were obtained by PCR using human ZF21 as a template. FAK mutants were obtained by PCR using human FAK as a template. To prepare ZF21 or its mutant fused to the N terminus of Venus protein, m1Venus cDNA (provided by Dr. A. Miyawaki, RIKEN, Japan) was amplified by PCR and cloned into the SacII site of the pLenti6/V5-DEST vector (Invitrogen). To prepare FAK, Paxillin or Zyxin fused to the C terminus of Venus protein, m1Venus cDNA was amplified by PCR and cloned into the SpeI site of the pLenti6/V5-DEST vector. To prepare Zyxin fused to the C terminus of monomeric cherry protein (mCherry), mCherry cDNA (provided by Dr. R. Tsien, Howard Hughes Medical Institute, University of California, San Diego) was amplified by PCR and cloned into the SpeI site of the pLenti6/V5-DEST vector. To express proteins for each experiment, the mammalian expression vector pLenti6/V5-DEST or the *E. coli* expression vector pDEST15 (Invitrogen) was used.

Knockdown Experiments Using shRNA—shRNA sequences used for knockdown of target proteins were as follows: ZF21, 5′-caccgcagtgtgacgccaagtttgacgaatcaaacttggcgtcacactgc-3′; FAK1, 5′-caccgcatcttccagttacaaattccgaagaatttgtaactggaagatgc-3′, and FAK2, 5′-caccgccaacccatctgatggaagacgaatcttccatcagatgggttggc-3′. shRNA expressing lentiviral vectors were generated and used according to the manufacturer's instructions (Invitrogen). For rescue experiments of ZF21 knockdown, an expression construct encoding a mutant ZF21 mRNA refractory to shRNA was generated by site-directed mutagenesis, and the mutant protein was expressed with a Myc tag at the C terminus using the pENTR vector (Invitrogen).

Immunofluorescence Microscopy—Cells were fixed in −20 °C methanol for 10 min and permeabilized using 0.1% Triton X-100 in PBS for 10 min. After the samples were blocked in PBS containing 5% goat serum and 3% bovine serum albumin, they were incubated with primary antibodies. All primary antibodies were visualized with either an Alexa 488- or 568-conjugated goat anti-mouse or anti-rabbit antibody (Invitrogen). Images of cells were captured with Leica ASMDW with CCD camera (Leica).

Cell Fractionation—Cells were homogenized in a buffer containing 250 mM sucrose and 25 mM Tris-HCl, pH 7.5. After centrifugation at 8,000 × *g* for 15 min, the supernatants were centrifuged further at 105,000 × *g* for 1 h. The pellet was used as the membrane fraction and the supernatant as the cytoplasmic fraction.

Adhesion Assay—For the cell adhesion assay, the surface of 12-well plates was coated with poly-L-lysine, fibronectin, collagen I, or vitronectin at a concentration of 1 μg/ml, and nonspecific binding sites were blocked with 0.5 mg/ml bovine serum albumin. Cells suspended in serum-free DMEM were seeded onto the plates at 3×10^4 cells per well and incubated for 30 min. After removal of nonadherent cells, adherent cells were trypsinized and counted.

The effect of blocking of integrin-β1 on cell adhesion was analyzed as follows. 96-Well plates were coated with poly-L-lysine, collagen I, fibronectin, or vitronectin (1 μg/ml), and nonspecific binding sites were blocked with 0.5 mg/ml bovine serum albumin. Cells suspended in serum-free DMEM were seeded onto the wells (2×10^4 cells per well) and incubated for 30 min in the presence or absence of 1 μg/ml integrin-β1 blocking antibody. After removal of nonadherent cells by washing, the remaining cells were stained with Hoechst 33342. Finally, fluorescence was quantified in a FLUOstar OPTIMA (BMG LABTECH).

Cell Migration Assay—Both sides of transwells with 8-μm pore size filters (Corning Glass) were precoated with fibronectin (5 μg/ml) for 1 h at 37 °C. DMEM (400 μl) containing 10% fetal bovine serum was added to the lower chamber, and 200 μl of a cell suspension (5×10^4 cells) was placed in the upper chamber. The plates were incubated at 37 °C in a 5% CO_2 atmo-

[3] M. Nagano, D. Hoshino, T. Sakamoto, N. Kawasaki, N. Koshikawa, and M. Seiki, unpublished results.

sphere for 6 h. Cells in the lower chamber were then stained with 0.5% crystal violet solution and counted using a light microscope at ×200 magnification. Values are averages of three fields.

Cell Surface Protein Pulldown Assay—A pulldown assay of cell surface proteins was performed as described previously (33). Briefly, cells were washed three times with chilled PBS containing 1 mM $MgCl_2$ and 0.1 mM $CaCl_2$ and then incubated with sulfo-NHS-biotin (Pierce) (0.1 mg/ml) in the same buffer at 4 °C for 30 min. The reaction was terminated by incubating the cells with 100 mM glycine in PBS. The cells were lysed in TNETS buffer (25 mM Tris-HCl, pH 7.5, 150 mM NaCl, 2 mM EDTA, 1% Triton X-100, 1% SDS), and the biotinylated proteins were precipitated with streptavidin-conjugated Sepharose beads (Amersham Biosciences). The samples were analyzed by Western blot using each antibody.

TIRF Microscopy—For TIRF microscopy, living cells were observed using an APON 60×OTIRFM objective on an IX81 microscope equipped with a TIRF illuminator and fiber optic coupled laser illumination (Olympus).

Immunoprecipitation—Cells were lysed with immunoprecipitation buffer (1% Nonidet P-40, 50 mM Tris-HCl, pH 7.4, 150 mM NaCl, 2 mM $MgCl_2$, 1 mM EGTA, 1 mM Na_3VO_4, and protease inhibitor mixture Set III). Endogenous ZF21 in the lysate was captured with chicken anti-ZF21 IgY and immunoprecipitated using chicken IgY precipitating agarose beads (Millipore). Venus-tagged proteins were immunoprecipitated using agarose beads conjugated to anti-GFP antibody (MBL). The beads were washed three times with immunoprecipitation buffer, and bound proteins were eluted with Laemmli sample buffer.

Pulldown Assay—Cells cultured on a plastic plate were washed with ice-cold PBS and scraped off in RIPA buffer (50 mM Tris-HCl, pH 7.5, 100 mM NaCl, 2 mM $MgCl_2$, 0.1% SDS, 0.5% sodium deoxycholate, 1% Triton X-100, 10% glycerol, 1 mM Na_3VO_4, and protease inhibitor mixture Set III) on ice. Lysates were centrifuged for 5 min at 20,000 × *g* at 4 °C. A fraction of the cleared lysates was incubated with 10 μg of GST-ZF21 or GST-ZF21 mutant bound to glutathione-conjugated Sepharose beads at 4 °C for 6 h. Pellets containing the beads were collected, washed three times with ice-cold RIPA buffer, and subjected to SDS-PAGE followed by Western blot analysis using the indicated antibodies.

Hypo-osmotic Shock—Hypo-osmotic shock for cells was performed as described previously (34). Briefly, cells were grown 48 h on 10-cm dishes. Cells were washed with PIPES buffer (20 mM PIPES, 100 mM KCl, 5 mM $MgCl_2$, 3 mM EGTA, pH 6.0) and exposed to a hypo-osmotic condition in 20% PIPES buffer for 10 min. After the cells were disrupted, most cellular contents were removed and washed with PIPES buffer, pH 7.0. The adhesion plaques remaining on the dish were resolved with Laemmli sample buffer and analyzed by Western blot using each antibody.

Focal Adhesion Disassembly Assay—The focal adhesion disassembly assay was performed as described previously (23). Briefly, cells were grown on fibronectin-coated glass coverslips and treated with 5 μM nocodazole for 30 min to depolymerize microtubules. After the drug was removed, cells were incubated to resume polymerization of microtubules. Cells were fixed in −20 °C methanol for 10 min, rehydrated in PBS followed by permeabilizing with 0.1% Triton-X100 in PBS for 5 min, and subjected to immunohistochemistry.

FAK Dephosphorylation Assay—The FAK dephosphorylation assay was performed as described previously (23). Briefly, cells were grown on fibronectin-coated plastic dishes and treated with 5 μM nocodazole for 30 min to depolymerize microtubules. After the drug was removed, cells were incubated to resume polymerization of microtubules. Cells were resolved with Laemmli sample buffer and analyzed by Western blot analysis.

Statistical Analysis—Data represent the means ± S.D. The unpaired Student's *t* test was used for analyzing differences between experimental groups.

RESULTS

FYVE Domain of ZF21 Mediates Membrane Localization—ZF21 is a member of a protein family characterized by the presence of a Fab1p-YOPB-Vps27p-EEA1 (FYVE) domain (35), which binds phosphatidylinositol 3-phosphate within the plasma membrane but contains no other previously described functional motifs (Fig. 1*A*). The FYVE domain-containing family of proteins includes 38 members that only exhibit conserved amino acid sequences within this FYVE domain. This finding suggests that family members exhibit divergent functions, and certain of these proteins have been shown to modulate signaling processes, membrane trafficking, or cytoskeletal reorganization (36). Two isoforms of ZF21 are predicted (encoding 234 or 252 amino acids) based on the presence of two mRNA splice variants. ZF21 mRNAs are expressed nearly ubiquitously in mouse tissues (supplemental Fig. S1*A*). We detected the shorter variant of the ZF21 protein in all human cell lines that we analyzed by Western blot, whereas the expression of the longer variant was more variable and not always present (supplemental Fig. S1*B*). In the following experiments, we studied the shorter variant ZF21(WT) and a mutant thereof (HN) containing two amino acid substitutions in the consensus sequence for binding phosphatidylinositol 3-phosphate (Fig. 1*A*) (37, 38).

We detected expression of the endogenous ZF21 in human fibrosarcoma-derived HT1080 cells as a 27-kDa protein by Western blot analysis using a polyclonal antibody generated against the recombinant protein (Fig. 1*B*). Biochemical fractionation of the cells revealed that ZF21 was enriched in the plasma membrane fraction, as was the transferrin receptor used as a positive control membrane protein, although we did detect some expression of ZF21 in the cytoplasmic fraction (Fig. 1*B*). To examine whether the FYVE domain is crucial for membrane association, we first created fusion proteins comprising the m1Venus protein fused to the C terminus of ZF21(WT) or ZF21(HN) and stably expressed these fusions in HT1080 cells. We used a lentiviral vector to express the exogenous proteins and to knock down expression of the endogenous proteins using shRNAs. Although the m1Venus-tagged ZF21(WT) was enriched in the membrane fraction, the m1Venus-tagged ZF21(HN) protein was not (Fig. 1*C*), suggesting that the FYVE domain is important for membrane localization. Immunohistochemical analysis of the subcellular localization of m1Venus-

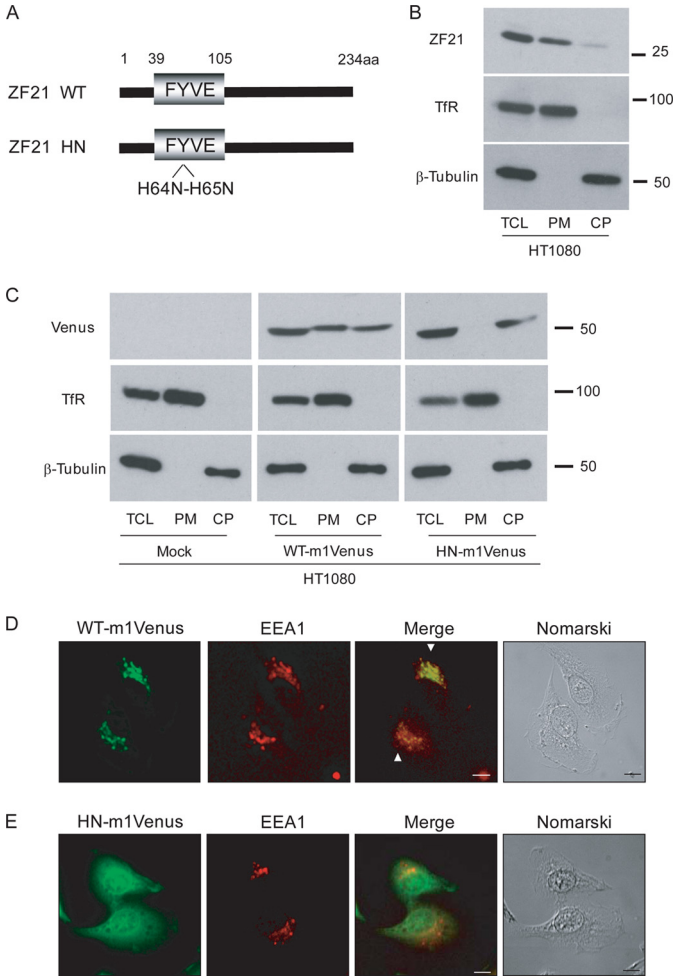

FIGURE 1. **ZF21 protein associates with the plasma membrane via the FYVE domain.** *A,* schematic representation of ZF21(WT) and ZF21(HN) proteins. *aa*, amino acids. *B,* localization of ZF21 in the plasma membrane fraction. HT1080 cells were homogenized and separated into membrane and cytoplasmic fractions. Endogenous ZF21 was detected by Western blot analysis using anti-ZF21 antibody. Transferrin receptor (*TfR*) and β-tubulin represent markers for membrane and cytoplasmic proteins, respectively. *TCL*, total cell lysate; *PM*, plasma membrane; *CP*, cytoplasmic proteins. *C,* association of ZF21 with the plasma membrane via the FYVE domain. WT ZF21 and its mutant were expressed in HT1080 cells as m1Venus-tagged forms (WT-m1Venus and HN-m1Venus, respectively) and analyzed similarly. *D* and *E,* HT1080 cells stably expressing either WT-m1Venus (*D*) or HN-m1Venus (*E*) were cultured in 4-well chamber plates. *EEA1*, an endosome marker, was visualized with anti-EEA1 followed by a secondary antibody conjugated to Alexa Fluor 568 (*red*). *Arrowheads* (*D*) indicate ZF21 co-localized with EEA1. HN-m1Venus was distributed within the cytoplasm and did not co-localize with EEA1 (*E*). CCD images using a ×60 objective lens (*scale bar,* 10 μm) are shown.

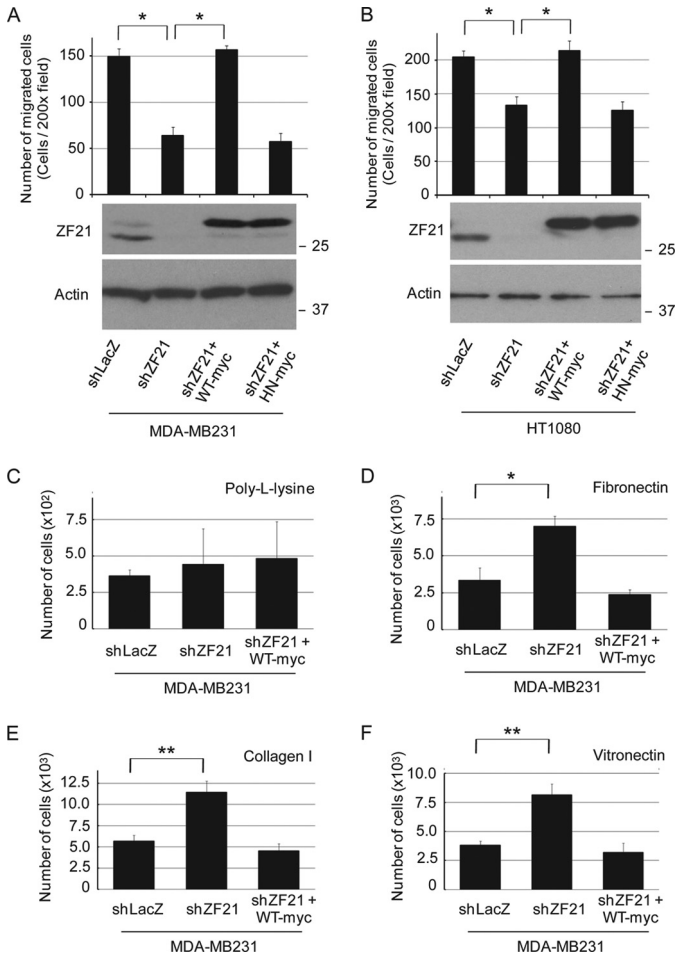

FIGURE 2. **ZF21 regulates adhesion to the ECM and cell migration.** *A* and *B,* expression of ZF21 was knocked down using shRNA (shZF21) in MDA-MB231 (*A*) or HT1080 (*B*) cells. To rule out off-target effects of shZF21, ZF21-myc (WT-myc) or ZF21(HN)-myc mutant (HN-myc) was expressed in the knockdown cells. The cells were subjected to a migration assay using a transwell chamber equipped with filters coated with fibronectin, and fetal bovine serum was used as an attractant. *Error bars* indicate the means ± S.D. ($n = 3$). *, $p < 0.005$ (Student's *t* test). The level of ZF21 expression was detected by Western blot analysis as presented in the *bottom panels*. *C–F,* MDA-MB231 cells used for migration assays in *A* were plated onto 12-well plates (3×10^4 cells per well) coated with poly-L-lysine (*C*), fibronectin (*D*), collagen I (*E*), or vitronectin (*F*) and incubated for 30 min. Adherent cells were then counted. *Error bars* indicate the means ± S.D. ($n = 3$). *, $p < 0.01$; **, $p < 0.005$ (Student's *t* test).

tagged ZF21(WT) (WT-m1Venus) revealed a vesicle-like distribution of the signal within the cells (*arrowheads*), most of which co-localized with EEA-1, a marker protein for endosomes (Fig. 1*D*). In contrast, a similar analysis of the m1Venus-tagged FYVE domain mutant (HN-m1Venus) revealed a more diffuse cytoplasmic localization (Fig. 1*E*).

ZF21 Affects Cell Motility by Regulating Cell Adhesion—We next observed that constitutive knockdown of the expression of ZF21 reduced the rate of migration of MDA-MB231 (Fig. 2*A*) and HT1080 (Fig. 2*B*) cells. However, forced expression of a Myc-tagged wild type ZF21 (WT-myc) in cells in which expression of ZF21 had been knocked down restored cell migration, whereas forced expression of a Myc-tagged HN mutant (HN-myc) in such cells did not.

The cells in which expression of ZF21 had been knocked down following expression of the shRNA showed reduced motility and exhibited more adherent morphology on the culture dish compared with the control cells. This suggested to us that ZF21 might regulate cell adhesion and thereby affect cell motility. To test this, MDA-MB231 cells that had been transduced with the shZF21- or control shLacZ-expressing vectors were suspended and seeded on plastic plates that had been coated with different ECM of proteins. Adhesion of the cells to poly-L-lysine was unaffected by knockdown of ZF21 expression (Fig. 2*C*). However, adhesion of the cells to fibronectin, collagen I, and vitronectin was enhanced significantly following shRNA-mediated knockdown of the expression of ZF21 (shZF21), compared with the cells expressing the irrelevant control shRNA

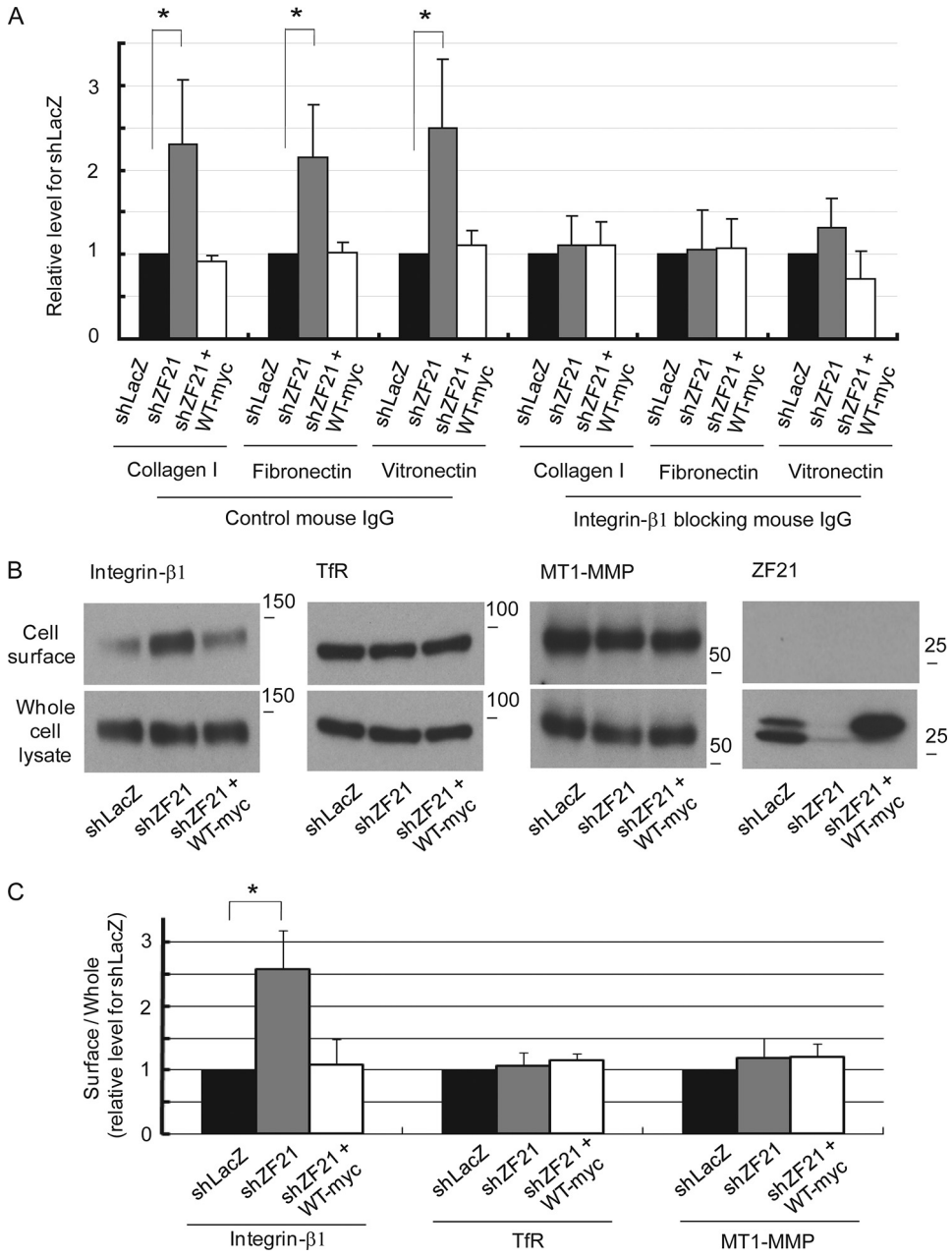

FIGURE 3. **ZF21 regulates the level of integrin-β1 expressed on the surface of the cell.** *A,* ZF21 regulates cell adhesion mediated by integrin-β1. MDA-MB231 cells prepared as in Fig. 2 were seeded onto 96-well plates (2×10^4 cells per well) coated with 1 μg/ml collagen I, fibronectin, or vitronectin and incubated for 30 min in the presence or absence of an anti-integrin-β1 blocking antibody. The adherent cells were stained with Hoechst 33342. The fluorescence was quantified in a FLUOstar OPTIMA (BMG Labtech). *Error bars* indicate the means ± S.D. ($n = 4$). *, $p < 0.05$ (Student's *t* test). *B,* detection of proteins expressed on the surface of the cells. Expression of the indicated proteins in the same set of MDA-MB231 cells was analyzed by Western blot analysis using whole cell lysate (*left*). Proteins on the surface of cells were labeled with biotin, affinity-purified, and analyzed similarly (*right*). *TfR*, transferrin receptor. *C,* quantification of the levels of protein detected in *B* ($n = 3$). The experiment in *C* was repeated three times, and the intensity of the antibody signals was quantified. The relative amount of each protein to that observed in the control cells is presented. *, $p < 0.05$ (Student's *t* test).

(shLacZ) (Fig. 2, *D–F*, respectively). Forced expression of WT-myc mitigated the enhanced cell adhesion observed in the ZF21 knockdown cells to a level observed in the cells expressing the control shRNA. These results indicated that ZF21 protein regulates adhesion of cells to ECM proteins.

ZF21 Increases Cell Surface Expression of Integrin-β1—Integrins are the major receptors for ECM components (4). We next made use of an antibody that blocks binding of integrin-β1 to the ECM so as to examine whether ZF21 affects integrin-mediated cell adhesion. The enhanced adhesion of the cells to collagen I, fibronectin, or vitronectin observed in the ZF21 knockdown cells was nearly fully suppressed by exposure of the cells to this blocking antibody (Fig. 3*A*).

We next analyzed the level of the integrin-β1 protein in whole cell lysates and in preparations of membrane proteins prepared from MDA-MB231 cells expressing either the control or ZF21 knockdown shRNA. The level of expression of integrin-β1 in whole cell lysates was unaffected following expression of either the control or ZF21-targeted shRNA vector or in cells also expressing the WT-myc fusion protein (Fig. 3*B*, *integrin-β1, lower panel*). To detect integrin-β1 expressed on the surface of these cells, proteins on the surface were labeled with biotin, affinity-purified using streptavidin beads, and subjected to Western blot analysis (Fig. 3*B*, *integrin-β1, upper panel*). The relative level of the expression of integrin-β1 on the cell surface *versus* the level in the whole cell lysate was quantified following repetition of the experiments and is presented in Fig. 3*C*. Cell surface expression of integrin-β1 was enhanced significantly following knockdown of the expression of ZF21, and expression of Myc-tagged ZF21 in the knockdown cells reduced integrin-β1 expression to a level similar to that observed in the control (shLacZ) cells (Fig. 3*C*). We concluded that ZF21 did not affect the cell surface expression of other membrane proteins, because its knockdown did not affect the level of biotin-labeled transferrin receptor or membrane type 1 matrix metalloproteinase (Fig. 3, *B* and *C*). Thus, ZF21 specifically regulates expression of integrin-β1 on the cell surface.

Knockdown of ZF21 Increases the Number of Focal Adhesions—Because integrin-β1 is an integral component of FAs, changes in the level of its membrane localization following knockdown of ZF21 might be due to effects of this knockdown on the formation and/or turnover of FAs. FAs were visualized by immunohistochemistry using antibodies against FA-resident proteins such as Vinculin, Talin, and FAK. MDA-MB231 cells

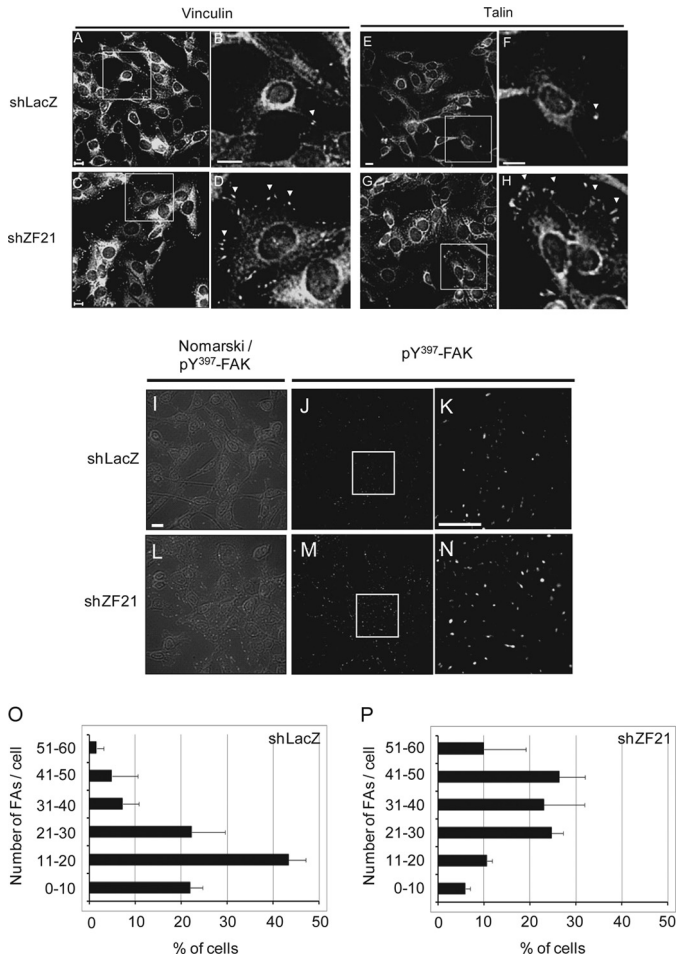

FIGURE 4. **ZF21 modulates focal adhesions.** *A–N,* FAs formed by MDA-MB-231 cells. Cells expressing shLacZ (*A, B, E, F,* and *I–K*) or shZF21 (*C, D, G, H, L,* and *M*) were seeded onto glass coverslips in 10% fetal bovine serum containing DMEM. After 48 h, Vinculin (*A–D*), Talin (*E–H*), or FAK phosphorylated at Tyr^{397} (*I–N*) was visualized with specific antibodies. The *boxed areas* in *A, C, E, G, J,* and *M* are shown at higher magnification in the panels in *B, D, F, H, K,* and *N*, respectively. *Scale bar,* 10 μm. *I* and *L* are merged images of immunostaining and images derived by Nomarski interference phase microscopy. *O* and *P,* quantitative analysis of the number of Tyr(P)^{397}-FAK dots. Number of FAs detected as Tyr(P)^{397}-positive dots per cell was counted for 100 cells, and the experiment was independently repeated three times.

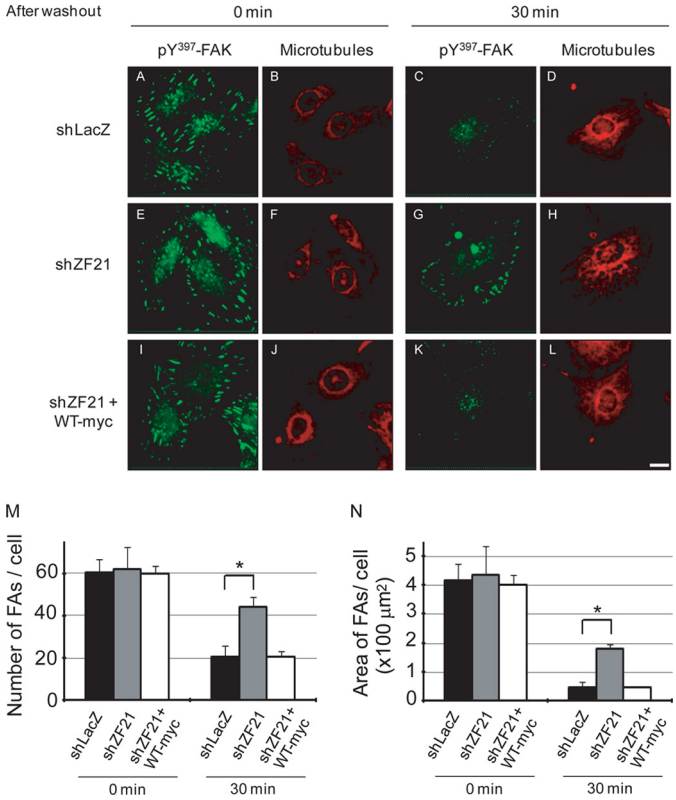

FIGURE 5. **ZF21 is required for disassembly of FAs.** *A–L,* immunostaining of MDA-MB-231 cells for Tyr(P)^{397}-FAK and microtubules. The same set of MDA-MB231 cells used in Fig. 3 was seeded onto fibronectin-coated glass coverslips. After 48 h, cells were treated with nocodazole (5 μM) for 30 min. Then the cells were washed and cultured with nocodazole-free media for 0 (*A, B, E, F, I,* and *J*) or 30 min (*C, D, G, H, K,* and *L*). The cells were subjected to immunostaining for Tyr(P)^{397}-FAK (*green, A, C, E, G, I,* and *K*) and microtubules (*red, B, D, F, H, J,* and *L*), respectively. Cells also expressed shLacZ (*A–D*), shZF21 (*E–H*), or shZF21 + WT-myc (*I–L*). *Scale bar,* 10 μm. *M* and *N,* quantitative analysis of FAs. Number of FAs per cell was counted for 30 cells in three separate experiments (*M*). Total area of FAs per cell was also measured (*N*). *Error bars* indicate the means ± S.D. *, $p < 0.01$; **, $p < 0.005$ (Student's *t* test).

expressing either the shLacZ or shZF21 vectors were cultured on a glass slide and subjected to immunohistochemistry using each antibody. Vinculin (Fig. 4, *A–D*) and Talin (Fig. 4, *E–H*) showed a punctate distribution at the periphery of the cells presumably representing Fas, and the areas enclosed by the *boxes* are enlarged in the *right panels*. The number of FA-like punctates appeared to be increased in the ZF21 knockdown cells compared with the control cells. FAs were further visualized using an antibody that specifically recognizes FAK that is phosphorylated at Tyr^{397}. The immunohistochemical signal is presented both in a form overlaid upon the optical microscope image (Fig. 4, *I* and *L*) and alone (Fig. 4, *J* and *M*). This signal exhibited a punctate distribution similar to that of Vinculin and Talin. The areas enclosed by the *boxes* in Fig. 4, *J* and *M,* are enlarged in Fig. 4, *K* and *N*, respectively. The number of FAs was counted and compared between control (*shLacZ,* Fig. 4*O*) and ZF21 knockdown (*shZF21,* Fig. 4*P*) cells. The average number of FAs per cell was significantly increased in the knockdown cells compared with the number observed in the control cells. Thus, the effect of ZF21 on the amount of integrin-β1 expressed on the cell surface likely reflects an effect of ZF21 protein upon the formation and/or disassembly of FAs.

ZF21 Regulates Disassembly of FAs—ZF21 presumably affects the level of FAs by modulating either their formation or disassembly. Treatment of cells with nocodazole disrupts microtubules and stabilizes FAs by preventing their disassembly (23). Subsequent depletion of the drug restores microtubules and triggers the synchronous disassembly of FAs. To identify the ZF21-dependent regulatory step in relation to the nocodazole-sensitive step, we treated MDA-MB231 cells expressing shLacZ, shZF21, or shZF21 + Myc-tagged ZF21 with nocodazole. Nocodazole treatment of the cells disrupted fibrous microtubule structures as confirmed by immunostaining of the cells with an antibody against microtubules (Fig. 5, *B, F,* and *J*). FAs were visualized by immunostaining with an antibody recognizing Tyr(P)^{397}-FAK, and the level of expression of ZF21 did not affect the number of FAs observed in cells treated with nocodazole (Fig. 5, *A, E,* and *I* for images and *M* and *N* for quantification). These results indicate that ZF21 did not affect formation of FAs and instead suggested that it might

regulate disassembly of FAs at some step after the nocodazole-dependent step. Subsequent depletion of nocodazole from the culture media and 30 min of incubation induced re-formation of microtubule structures as confirmed by immunostaining (Fig. 5, *D, H,* and *L*). The number of FAs in the control cells decreased markedly as observed in Fig. 5, *C* and *M*. In parallel with the decrease in the number of FAs, the area covered by the FAs also decreased (Fig. 5*N*, *shLacZ*). In contrast, the decrease in the number of FAs (Fig. 5, *G* and *M*) and in the area covered by the FAs (Fig. 5*N*) was significantly delayed in cells in which expression of ZF21 was knocked down. Thus, ZF21 appears to play a role during microtubule-induced disassembly of FAs.

ZF21 Is a Component of Focal Adhesions—Because ZF21 regulates turnover of FAs, we examined whether ZF21 is a component protein of FAs in MDA-MB231 cells expressing m1Venus-tagged ZF21. Although most ZF21 protein is associated with intracellular vesicles (Fig. 1*D*), at least some fraction of ZF21 showed co-localization with Talin at the periphery of the cells (Fig. 6*A*). To capture live images of ZF21 localized to sites of adhesion of the cell to the ECM, we employed TIRF microscopy, with which we could visualize only fluorescence-labeled proteins located in the vicinity of sites of cell attachment to the slide glass in response to localized activation with a laser beam. We made use of mCherry-tagged Zyxin as a marker for FAs (Fig. 6*B*, *red*), although ZF21 was monitored by the fluorescence of the m1Venus tag (Fig. 6*B*, *green*). We observed co-localization of the fluorescent signals associated with the tagged ZF21 and Zyxin indicating that ZF21 localizes to FAs.

FAs include multiple components that interact to both form the physical structure of FAs and to transduce signals. To test whether ZF21 interacts with other FA components, we performed a pulldown assay using a glutathione *S*-transferase (GST)-fused ZF21 protein. FAK, Paxillin, or Zyxin was expressed in COS-1 cells as m1Venus-tagged forms. We observed binding of FAK, but not Paxillin or Zyxin, to GST-ZF21 based on Western blot analysis of proteins pulled down with the GST-ZF21 (Fig. 6*C*). We were also unable to pull down other proteins, such as Talin, Vinculin, or α-actinin by this same GST-ZF21 pulldown assay.[3]

To delineate FAK domains that mediate binding to ZF21, we expressed various deletion constructs of FAK in COS-1 cells as fusions with a V5 tag. Cell lysates were prepared and subjected to a pulldown assay using GST-ZF21 as bait (Fig. 6*D*). An N-terminal fragment that lacks the kinase domain and FAT domain failed to bind ZF21 (Fig. 6*D*, *FERM*). In contrast, the kinase domain of FAK alone was sufficient to bind ZF21 (Fig. 6*D*, *KD*). Similarly, we analyzed the binding of ZF21 domains to FAK using the GST-fused deletion mutants (Fig. 6*E*). N- and C-terminal fragments of ZF21 showed a greatly reduced ability to bind FAK, whereas the FYVE domain alone was sufficient to bind FAK (Fig. 6*E*).

We next tested whether the interaction between FAK and ZF21 might play a role in sequestering the latter in FAs. To test this idea, MDA-MB231 cells adhering to a culture dish were disrupted under hypo-osmotic conditions, which allows most intracellular components to separate from the attached membrane fraction (34). Residual membrane fragments containing FAs were solubilized and subjected to Western blot analysis (Fig. 6*F*). EEA1, an endosomal protein, was largely absent from the residual membrane fragments after hypo-osmotic treatment of the cells compared with the untreated cells (Fig. 6*F*, *4th lane*). In contrast, FAK and integrin-β1 were detected in the residual membrane fragments even after hypo-osmotic treatment of the cells (Fig. 6*F*, *4th lane*). Similarly to FAK and integrin-β1, endogenous ZF21 protein was detected in the residual fraction adhering to the dishes (Fig. 6*F*, *4th lane*). However, ZF21 was not detected in the residual adherent fraction of the cells if FAK expression was knocked down using shRNA (Fig. 6*F*, *2nd* and *3rd versus 5th* and *6th lanes*). This is not because knockdown of FAK expression destroyed whole cell adhesion structures, because a comparable amount of integrin-β1 was retained in the residual fraction of the knockdown cells (Fig. 6*F*, *5th* and *6th lanes*) as was observed in the control cells (Fig. 6*F*, *4th lane*).

ZF21 Regulates Microtubule-dependent Dephosphorylation of Tyr(P)^{397}-FAK—Dephosphorylation of FAK at Tyr(P)^{397} is crucial for the induction of FAs disassembly (39). Therefore, we tested whether ZF21 regulates dephosphorylation of FAK. MDA-MB231 cells expressing shLacZ, shZF21, or shZF21 + Myc-tagged ZF21 were treated with nocodazole, and the level of Tyr(P)^{397}-FAK was monitored by Western blot analysis of cell lysates prepared after removal of the drug (Fig. 7*A*). Quantitative measurement of the level of phosphorylated FAK was carried out and is presented in Fig. 7*B*. The level of Tyr(P)^{397}-FAK in the control cells (shLacZ) was decreased following removal of nocodazole and reached 20% of the original level within 15 min (Fig. 7, *A* and *B*). In contrast, the decrease in phosphorylation of FAK was significantly delayed in the ZF21 knockdown cells (shZF21), retaining a level of phosphorylation equivalent to ~60% of the original level even after 30 min. The effect of knockdown of shZF21 on FAK phosphorylation was reversed completely by expression of the Myc-tagged ZF21.

However, the decrease in the level of Tyr(P)^{397}-FAK after the re-growth of microtubules may reflect preferential degradation of the phosphorylated FAK rather than dephosphorylation. To exclude this possibility, we repeated the experiments in Fig. 7*A* in the presence of the phosphatase inhibitor, vanadate (Fig. 7*C*), and we found that vanadate inhibited the decrease in the level of Tyr(P)^{397}-FAK. Thus, ZF21 regulates the microtubule-induced dephosphorylation of FAK, and protein-tyrosine phosphatases such as SHP-2 and PTP-1B, which are reported to induce dephosphorylation of FAK (28, 29), may be involved in this process. We examined whether these phosphatases associate with ZF21 and FAK by immunoprecipitating ZF21, and we observed co-precipitation of endogenous FAK and SHP-2, but not PTP-1B, by Western blot analysis (Fig. 7*D*). Thus, SHP-2 likely acts on FAK during microtubule-induced disassembly of FAs.

DISCUSSION

In this study, we identified ZF21 to be a regulator of adhesion to and migration on the ECM. Reduced expression of ZF21 led to enhanced adhesion to the ECM by preventing disassembly of FAs, thereby suppressing cell migration. ZF21 and FAK interact

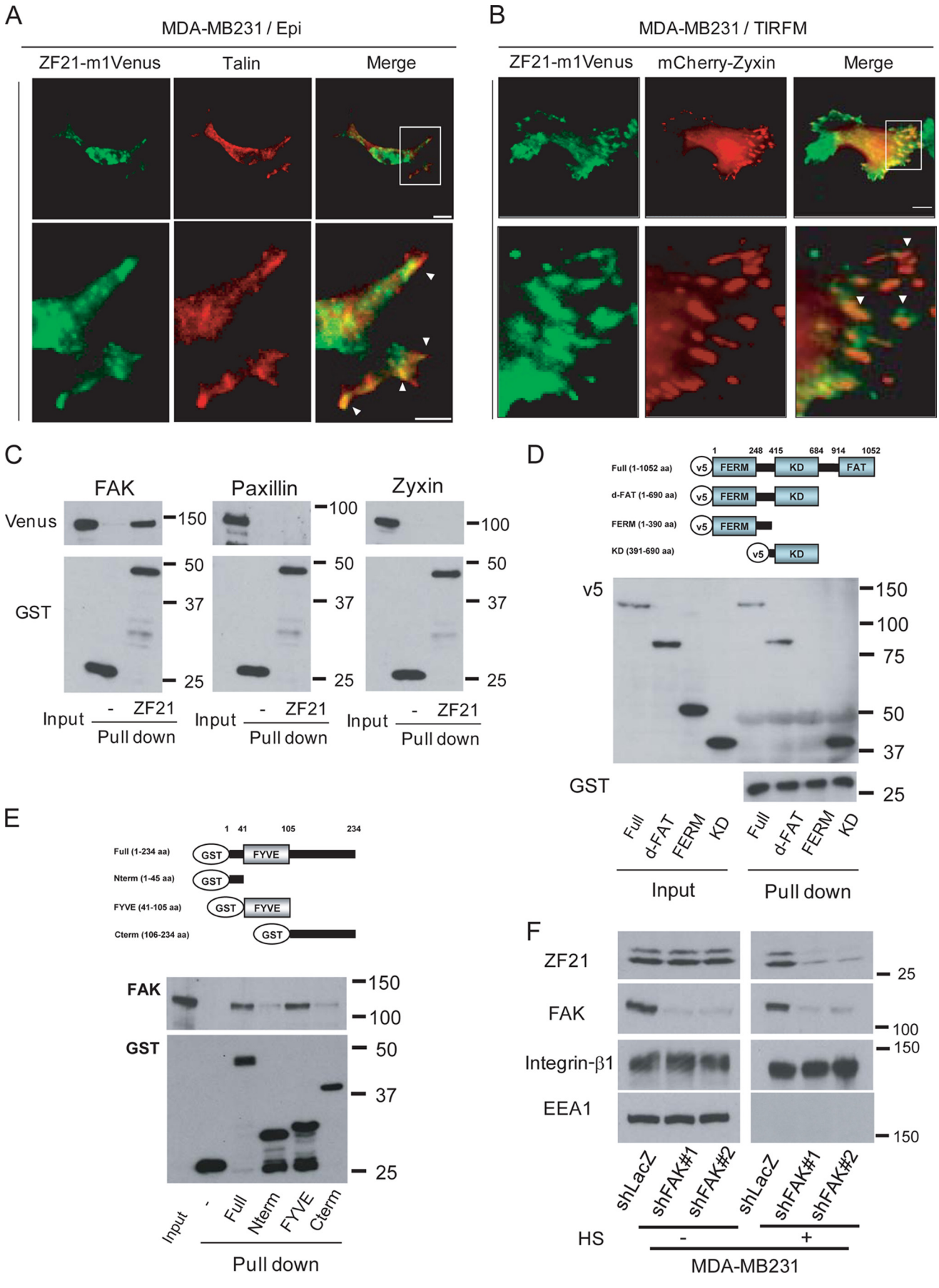
A
MDA-MB231 / Epi
ZF21-m1Venus
Talin
Merge
B
MDA-MB231 / TIRFM
ZF21-m1Venus
mCherry-Zyxin
Merge
C
FAK
Paxillin
Zyxin
Venus
GST
150
100
50
37
25
Input
-
ZF21
Pull down
D
Full (1-1052 aa)
d-FAT (1-690 aa)
FERM (1-390 aa)
KD (391-690 aa)
v5
FERM
KD
FAT
1
248
415
684
914
1052
150
100
75
50
37
25
Full
d-FAT
FERM
KD
Input
Pull down
E
Full (1-234 aa)
Nterm (1-45 aa)
FYVE (41-105 aa)
Cterm (106-234 aa)
GST
FYVE
1
41
105
234
FAK
150
100
50
37
25
Input
-
Full
Nterm
FYVE
Cterm
Pull down
F
ZF21
FAK
Integrin-β1
EEA1
25
100
150
150
shLacZ
shFAK#1
shFAK#2
HS
-
+
MDA-MB231

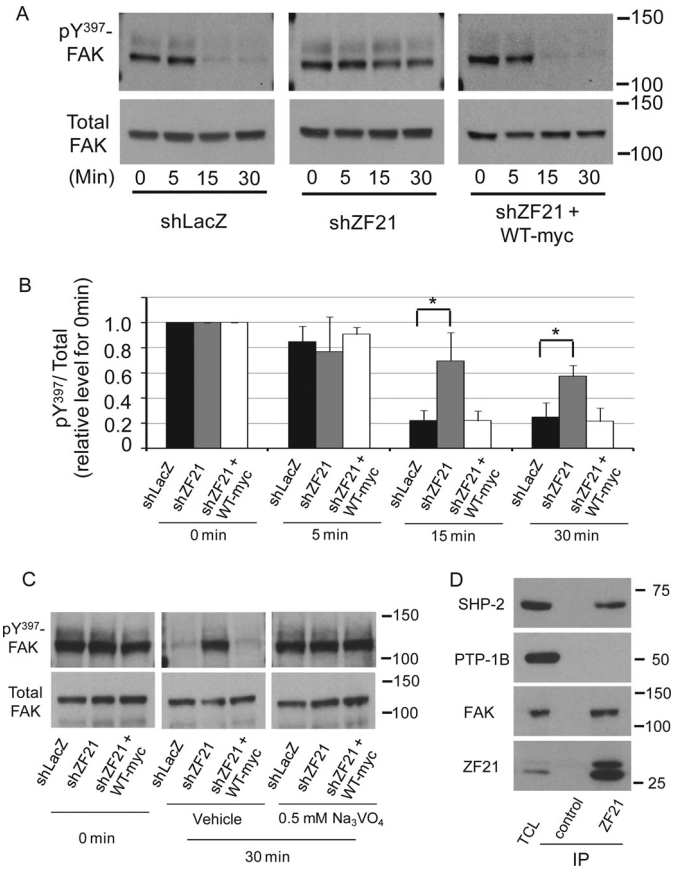

FIGURE 7. **Knockdown of ZF21 suppresses the microtubule-induced reduction in Tyr(P)^{397}-FAK.** *A,* dephosphorylation of Tyr(P)^{397}-FAK in nocodazole-treated MDA-MB-231 cells. The same set of cells used in Fig. 3 was subjected to the analysis. Cell lysates were prepared at the indicated time points after deprivation of nocodazole. Total FAK and Tyr(P)^{397}-FAK were detected by Western blot analysis. *B,* experiments in *A* were repeated three times ($n = 3$), and the intensities of the bands were quantified. Relative levels of Tyr(P)^{397}/total FAK to those at 0 min are presented. *, $p < 0.05$ (Student's *t* test). *C,* phosphatase dependence of the dephosphorylation of Tyr(P)^{397}-FAK in nocodazole-treated MDA-MB-231 cells. The same set of cells used in *A* was subjected to the analysis. Cell lysates were prepared just after deprivation of nocodazole or after the further incubation for 30 min in the presence or absence of 0.5 mM Na_3VO_4 after deprivation of nocodazole. Total FAK and Tyr(P)^{397}-FAK were detected by Western blot analysis. *D,* immunoprecipitation assay for endogenous ZF21 in MDA-MB231 cells. The lysates of MDA-MB231 cells were incubated with chicken anti-ZF21 IgY. The chicken anti-ZF21 IgY was precipitated with chicken IgY-precipitating agarose beads (Millipore). Proteins bound to ZF21 were analyzed by Western blotting using each antibody.

either directly or indirectly through specific domains, and this interaction is presumably important for recruitment of ZF21 to sites of cell adhesion. ZF21 is required for the microtubule-induced dephosphorylation of Tyr(P)^{397}-FAK at Fas, and therefore reduced expression of ZF21 prevents the disassembly of FAs.

ZF21 localizes to the plasma membrane via two different mechanisms. The FYVE domain of ZF21 contains a consensus sequence motif that binds phosphatidylinositol 3-phosphate within the lipid layer of the membrane. Amino acid substitutions in the FYVE domain of ZF21 abolish its ability to associate with the plasma membrane and cytoplasmic vesicles. In addition to this association with numerous intracellular vesicles, ZF21 protein also localizes to FAs, as we observed using TIRF microscopy to visualize proteins in close proximity to cell attachment sites on the slide glasses (Fig. 6*B*). We used a pulldown assay to show that ZF21 can bind FAK but not Paxillin or Zyxin (Fig. 6*C*). The FYVE domain of ZF21 is important not only for the localization to endosomes but also for the binding to FAK (Fig. 6*E*). Enrichment of ZF21 at sites of cell attachment was further confirmed by analyzing membrane fragments attached to the culture dish after removal of most cellular material following exposure of the cells to hypo-osmotic conditions (Fig. 6*F*). Enrichment of ZF21 to these sites of attachment was dependent on the presence of FAK.

Extension of microtubules to FAs induces disassembly of their structure (23, 24). Presumably, microtubules convey critical protein components that trigger disassembly of FAs. Kinesin-1, which is a motor protein that transports vesicles toward the plus end of microtubules, is reported to be necessary for the disassembly of FAs (25). Because ZF21 associates with endosomes, ZF21 and its associated proteins may act as triggers for the microtubule-induced disassembly of FAs.

Knockdown of ZF21 in cultured cells did not affect the number of FAs in cells treated with nocodazole. These results indicate that ZF21 does not affect the formation of FAs. Successive depletion of the drug from the culture media induced disassembly of FAs and consequently decreased the number of FAs in control cells. However, knockdown of ZF21 expression in the cells prevented this decrease in FAs in response to nocodazole depletion, indicating that ZF21 plays a crucial role specifically in the disassembly of FAs after the microtubule-dependent step. This activity of ZF21 explains why we observed increased

FIGURE 6. **ZF21 is a component of focal adhesions and binds FAK.** *A* and *B,* localization of ZF21 at FAs. *A,* MDA-MB231 cells stably expressing ZF21-m1Venus were cultured in 4-well chamber plates. Talin, an endogenous FA marker, was visualized with anti-Talin antibody followed by a secondary antibody conjugated to Alexa Fluor 568 (*red*). *Boxed areas* are shown at a higher magnification below. Co-localization of ZF21 and endogenous Talin at FAs is indicated by the *arrowheads*. *B,* MDA-MB231 cells stably expressing both ZF21-m1Venus (*green*) and mCherry-Zyxin (focal adhesion resident protein, *red*) were cultured onto a 35-mm glass-based dish, and cell adhesion sites were specifically visualized by total internal reflection fluorescence microscope (*TIRFM*). *Boxed areas* are shown at a higher magnification below. Co-localization of ZF21 and Zyxin at FAs is indicated by the *arrowheads*. *C,* pulldown assay of FA proteins using GST-ZF21. Whole cell lysates of COS-1 cells expressing either m1Venus-FAK, -Paxillin, or -Zyxin were incubated with GST-ZF21 or GST alone. Proteins bound to GST-ZF21 or GST were analyzed by Western blotting using anti-Venus or anti-GST antibody. *D,* pulldown assay of FAK truncation mutants using GST-ZF21. The domain structures of v5-tagged FAK derivatives are shown in the *upper panel* as follows: full-length (*Full*), FERM and kinase domain (*d-FAT*), FERM domain (*FERM*), and kinase domain (*KD*). The amino acid (*aa*) positions are indicated. Whole cell lysates of COS-1 cells expressing each of the v5-tagged FAK derivatives were incubated with GST-ZF21. Proteins bound to GST-ZF21 were analyzed by Western blot using anti-v5 or anti-GST antibody. *E,* pulldown assay of FAK using GST-ZF21 truncation mutant. The domain structures of GST-tagged ZF21 derivatives are shown in the *upper panel* as follows: full-length (*Full*), N-terminal domain (*Nterm*), FYVE domain (*FYVE*), and C-terminal domain (*Cterm*). The amino acid positions are indicated. Whole cell lysates of HeLa cells were incubated with GST-ZF21 derivatives or GST alone. Proteins bound to GST-ZF21 were analyzed by Western blot using anti-FAK or anti-GST antibody. *F,* detection of proteins at cell adhesion sites. To detect ZF21 at cell adhesion sites, MDA-MB231 cells were subjected to hypo-osmotic shock (+*HS*), and residual cell fragments adhering to the dishes were collected for Western blot analysis. The control was the lysate of cells without hypo-osmotic treatment (−*HS*). Expression of endogenous FAK was knocked down using two different shRNAs (*shFAK#1* and *shFAK#2*).

cell adhesion and suppression of motility on ECM following the knockdown of expression of ZF21.

Disassembly of FAs requires the function of multiple proteins. Calpain-2 is required for the proteolytic degradation of components of FAs (26, 40). Calpain-4 is a regulatory subunit for calpain-1 or -2, and fibroblasts obtained from calpain-4-null mice exhibit accumulation of unusually large FAs, and the cells exhibit reduced motility (41). Dephosphorylation of FAK and association of FAK with dynamin are required to reduce the level of cell surface integrins via endocytosis (23). Fibroblasts derived from FAK-null mice formed numerous immature FAs, and the turnover of FAs was abrogated (42). Reflecting the abnormal turnover of FAs, the FAK-null cells showed a decreased rate of cell migration (42).

The level of Tyr(P)^{397}-FAK decreased rapidly during synchronized disassembly of FAs after release of cells from nocodazole treatment, and treatment of cells with vanadate, a protein-tyrosine phosphatase inhibitor, prevented this decrease. Protein-tyrosine phosphatases, such as SHP-2 or PTP-PEST, have been reported to be responsible for the dephosphorylation of Tyr(P)^{397}-FAK and to regulate the turnover of FAs (27, 28). ZF21 interacts with FAK and SHP-2 in MDA-MB231 cells, and knockdown of ZF21 expression abrogated the dephosphorylation of Tyr(P)^{397}-FAK following nocodazole treatment of cells. So ZF21 appears to regulate either the recruitment or activity of SHP-2 during microtubule-induced disassembly of FAs.

In conclusion, we report that ZF21 is a regulator of cell adhesion. Because ZF21 regulates turnover of FAs, it also regulates cell motility on ECM. Thus, ZF21 is a potential new target for the treatment of cells that exhibit elevated motility and invasion, such as malignant tumor cells.

Acknowledgments—We thank Dr. A. Miyawaki for kindly providing m1Venus cDNA clones and Dr. R. Tsien for kindly providing mCherry cDNA clones.

REFERENCES

1. Hynes, R. O., and Lander, A. D. (1992) *Cell* **68,** 303–322
2. Meighan, C. M., and Schwarzbauer, J. E. (2008) *Curr. Opin. Cell Biol.* **20,** 520–524
3. Gumbiner, B. M. (1996) *Cell* **84,** 345–357
4. Hynes, R. O. (2002) *Cell* **110,** 673–687
5. Liu, S., Calderwood, D. A., and Ginsberg, M. H. (2000) *J. Cell Sci.* **113,** 3563–3571
6. Lauffenburger, D. A., and Horwitz, A. F. (1996) *Cell* **84,** 359–369
7. Broussard, J. A., Webb, D. J., and Kaverina, I. (2008) *Curr. Opin. Cell Biol.* **20,** 85–90
8. Critchley, D. R. (2000) *Curr. Opin. Cell Biol.* **12,** 133–139
9. Burridge, K., and Chrzanowska-Wodnicka, M. (1996) *Annu. Rev. Cell Dev. Biol.* **12,** 463–518
10. Ridley, A. J., Schwartz, M. A., Burridge, K., Firtel, R. A., Ginsberg, M. H., Borisy, G., Parsons, J. T., and Horwitz, A. R. (2003) *Science* **302,** 1704–1709
11. Galbraith, C. G., and Sheetz, M. P. (1998) *Curr. Opin. Cell Biol.* **10,** 566–571
12. Ren, X. D., Kiosses, W. B., and Schwartz, M. A. (1999) *EMBO J.* **18,** 578–585
13. Geiger, B., Bershadsky, A., Pankov, R., and Yamada, K. M. (2001) *Nat. Rev. Mol. Cell Biol.* **2,** 793–805
14. Burridge, K., Turner, C. E., and Romer, L. H. (1992) *J. Cell Biol.* **119,** 893–903
15. Humphries, J. D., Wang, P., Streuli, C., Geiger, B., Humphries, M. J., and Ballestrem, C. (2007) *J. Cell Biol.* **179,** 1043–1057
16. Glück, U., and Ben-Ze'ev, A. (1994) *J. Cell Sci.* **107,** 1773–1782
17. Horwitz, A., Duggan, K., Buck, C., Beckerle, M. C., and Burridge, K. (1986) *Nature* **320,** 531–533
18. Iwahara, T., Akagi, T., Fujitsuka, Y., and Hanafusa, H. (2004) *Proc. Natl. Acad. Sci. U.S.A.* **101,** 17693–17698
19. Mitra, S. K., Hanson, D. A., and Schlaepfer, D. D. (2005) *Nat. Rev. Mol. Cell Biol.* **6,** 56–68
20. Mitra, S. K., and Schlaepfer, D. D. (2006) *Curr. Opin. Cell Biol.* **18,** 516–523
21. Westhoff, M. A., Serrels, B., Fincham, V. J., Frame, M. C., and Carragher, N. O. (2004) *Mol. Cell. Biol.* **24,** 8113–8133
22. Chrzanowska-Wodnicka, M., and Burridge, K. (1996) *J. Cell Biol.* **133,** 1403–1415
23. Ezratty, E. J., Partridge, M. A., and Gundersen, G. G. (2005) *Nat. Cell Biol.* **7,** 581–590
24. Kaverina, I., Krylyshkina, O., and Small, J. V. (1999) *J. Cell Biol.* **146,** 1033–1044
25. Krylyshkina, O., Kaverina, I., Kranewitter, W., Steffen, W., Alonso, M. C., Cross, R. A., and Small, J. V. (2002) *J. Cell Biol.* **156,** 349–359
26. Glading, A., Lauffenburger, D. A., and Wells, A. (2002) *Trends Cell Biol.* **12,** 46–54
27. Angers-Loustau, A., Côté, J. F., Charest, A., Dowbenko, D., Spencer, S., Lasky, L. A., and Tremblay, M. L. (1999) *J. Cell Biol.* **144,** 1019–1031
28. Yu, D. H., Qu, C. K., Henegariu, O., Lu, X., and Feng, G. S. (1998) *J. Biol. Chem.* **273,** 21125–21131
29. Zhang, Z., Lin, S. Y., Neel, B. G., and Haimovich, B. (2006) *J. Biol. Chem.* **281,** 1746–1754
30. Chao, W. T., and Kunz, J. (2009) *FEBS Lett.* **583,** 1337–1343
31. Uekita, T., Gotoh, I., Kinoshita, T., Itoh, Y., Sato, H., Shiomi, T., Okada, Y., and Seiki, M. (2004) *J. Biol. Chem.* **279,** 12734–12743
32. Itoh, Y., and Seiki, M. (2006) *J. Cell. Physiol.* **206,** 1–8
33. Itoh, Y., Takamura, A., Ito, N., Maru, Y., Sato, H., Suenaga, N., Aoki, T., and Seiki, M. (2001) *EMBO J.* **20,** 4782–4793
34. Carlucci, A., Gedressi, C., Lignitto, L., Nezi, L., Villa-Moruzzi, E., Avvedimento, E. V., Gottesman, M., Garbi, C., and Feliciello, A. (2008) *J. Biol. Chem.* **283,** 10919–10929
35. Stenmark, H., Aasland, R., Toh, B. H., and D'Arrigo, A. (1996) *J. Biol. Chem.* **271,** 24048–24054
36. Gillooly, D. J., Simonsen, A., and Stenmark, H. (2001) *Biochem. J.* **355,** 249–258
37. Gaullier, J. M., Ronning, E., Gillooly, D. J., and Stenmark, H. (2000) *J. Biol. Chem.* **275,** 24595–24600
38. Lee, S. A., Eyeson, R., Cheever, M. L., Geng, J., Verkhusha, V. V., Burd, C., Overduin, M., and Kutateladze, T. G. (2005) *Proc. Natl. Acad. Sci. U.S.A.* **102,** 13052–13057
39. Mañes, S., Mira, E., Gómez-Mouton, C., Zhao, Z. J., Lacalle, R. A., and Martínez-A, C. (1999) *Mol. Cell. Biol.* **19,** 3125–3135
40. Franco, S. J., Rodgers, M. A., Perrin, B. J., Han, J., Bennin, D. A., Critchley, D. R., and Huttenlocher, A. (2004) *Nat. Cell Biol.* **6,** 977–983
41. Dourdin, N., Bhatt, A. K., Dutt, P., Greer, P. A., Arthur, J. S., Elce, J. S., and Huttenlocher, A. (2001) *J. Biol. Chem.* **276,** 48382–48388
42. Iliæ, D., Furuta, Y., Kanazawa, S., Takeda, N., Sobue, K., Nakatsuji, N., Nomura, S., Fujimoto, J., Okada, M., and Yamamoto, T. (1995) *Nature* **377,** 539–544